ISSN 2278-7763

# Experimental study of heating of Non-Newtonian suspensions made of hard large sized spherical particles and Tylose solution flowing in a horizontal complex duct.

**[1]Benoît Fanou Zinsou FAGLA, [2]Michel GRADECK, [2]Michel LEBOUCHE**

**1. Laboratoire d'Energétique et de Mécanique Appliquée (LEMA), Ecole Polytechnique d'Abomey-Calavi/Université d'Abomey-Calavi 01 B.P. 2009 Cotonou (Bénin). E-mail: fbzfagla@yahoo.fr**

**2. Laboratoire d'Energétique et de Mécanique Théorique et Appliquée (LEMTA)** CNRS/ INPL / **UHP1, avenue de la forêt de Haye - BP 160 54504 Vandoeuvre-lès-Nancy cedex (France). E-mail: michel.gradeck@univ-lorraine.fr; E-mail : michel.lebouche@univ-lorraine.fr**

## ABSTRACT

In this paper we present the results of an experimental study of the thermal of Non-Newtonian pseudoplastic suspensions in a horizontal duct with complex geometry in the Agro-Food industry (A.F.I.). We highlighted a limitation in the development of the thermal boundary layer which increases with the volume fraction of rigid spheres. The study highlights, on one hand, the interdependence between hydrodynamic and thermal of suspensions of particles with an average diameter of about 4.4 mm and the aspect ratio (d / D> 0.13) and on the other hand, the convective effects of the particles (disturbance of the boundary layer) in flow in a duct made of variable geometry. This study allowed us to understand the mechanisms of heating the mixture from the wall, observing an improvement in the quality of heat transfer with the concentration of hard spheres and with the use of a duct with complex geometry.

**Keywords**: Solid-liquid, Suspensions, Spheres, Thermal, Volume fraction, Hydrodynamics.

## Nomenclature

### Latin notations

**$D_H$ :** Hydraulic diameter (m)
L **:** The length of the measuring section (m).
**$D_2$ :** Maximum diameter into the geometry downstream of the sudden enlargement (with $D_2$ = 0.04 m)
$T_m(z)$ : temperature of the mixture (K)

t : constante
z : abscissa (m)
b : parameter such as $b = -\frac{\partial K}{\partial T} / K$
$D_H$ : hydraulic diameter (m)
D: heating diameter of vein (m)
$D_1$: height of rectangular channel before enlargement
$D_2$ : Maximum diameter $D_2$ passing into the geometry downstream of enlargement abrupt ($D_2$ = 0.04 m)
K: consistency index,
$C_P$ : specific heat (W / kg K)

$T_P(z)$ :wall temperature (K)
$Z_R$: abscissa of the point of reattachment (m)
n : index structure
Reg : Metzner and Reed's generalized Reynolds number
t : constant
Te: temperature at the inlet of the heat exchanger (K)
$\overline{U}$ : flow velocity (m / s)

$Z_R$: abscissa of the point of reattachment (m)
$R^2$ : regression coefficient
r : the radius of the pipe (m)
$Re_{am}$: Reynolds number calculated based on the diameter before enlargement.
H : step height after enlargement (m)
h (z): convective heat transfer coefficient (W / $m^2$.K)
$\dot{M}$ : mass flow rate (kg / s)
$Q_v$ : volume flow $m^3$ / s
A (z): heat exchange surface between the input and the abscissa z,

### Greek notations

$\Delta P$ : pressure drop
Φ: spherical particles volume fraction

ISSN 2278-7763

$\mu_m$: viscosity at the temperature of the mixture
$\rho$: density of the fluid,
$\varphi_p$: imposed heat flux density to the wall
$\tau_p$: wall stress
$\mu_e$: viscosity of the fluid at the inlet of the wall
$\mu_p$: viscosity at the wall
$\lambda$: thermal conductivity of the fluid

**dimensionless numbers**

Reg: Metzner and Reed's generalized Reynolds number
Nu (z): local Nusselt number
$Nu_\infty$: Nusselt number asymptotic
Gz: Graetz number
$Nu_{D2max:}$: Nusselt number maximum at the abscissa of the point of reattachment

## 1. INTRODUCTION

In the Agro-Food industry new products are put on the market to satisfy the consumer. Aseptic and organoleptic quality of the food fluids charged of solid particles depends on how they are treated. They often loaded with solid particles (yogurt with pieces of fruit, jams, ...) that modify completely the hydrodynamics and thermal of flow of the carrier fluid. Factors affecting the transport and heat transfer of carrier fluids responsible have been identified; this is the case of the particle size, the particle concentration, the flow regime of the suspension rheological characteristics of carrier fluids , the hydraulic diameter and the ratio of fluid density to particle density. Studies conducted by authors such as Chhabra [1] , Cheng [2], and Kemblowski and Kolodziejski [3] and Takahashi [4] on the hydraulic transport of hard spheres allow now fully understand the problem of pressure drop in horizontal conduct. This transport is strongly linked to the two-phase flow regime. Studies on many problems such as the transfer of heat between the carrier fluid and hard spheres in ducts of variable geometry are solved thanks to the works on solid-liquid suspensions led by Hoareau [5]. Fundamental dimensionless of grandeur such as the Reynolds number, the Prandtl number Pr and the Nusselt number (Nu) are used. This is the case of the Nusselt number which reaches a low value at the separation point and then increases linearly to a maximum at slightly beyond the reattachment zone that corresponds to the thermal boundary layer based on the work of Fagla [6] et Fagla [7] **.** Downstream of the point of reattachment, the Nusselt number tends to the obtained value for a free-flowing. Other authors have also worked on solid-liquid two-phase flows Rhafiki [8]. They studied the storage and distribution of cold latent heat treating, in a manner essentially numerical, two-phase flows with solid-liquid phase change in an exchanger. Two types of the phase change materials were tested: ice slurry and stabilized grout. The ice slurry is a suspension composed of a carrier phase. To model the flows of ice slurry, they chose a coupled approach: temperature, ice fraction, based on the assumption of a thermodynamic equilibrium between the solid and liquid phases. The results from the model and the experiment are in good agreement. They are used to estimate a precise way the local heat exchange coefficient along the exchanger. In the case of stabilized grout, they proposed a physical and homogeneous 2D model describing the flow taking into account the heat transfers with phase change in a warming (melting of a pure substance and a binary solution (or cooling (crystallization of a pure substance). the model allows to determine the coefficient of heat exchange between the two-phase mixture and the wall of the exchanger. Finally, they developed a model based on two phases Eulerian approach. This one introduces coupling between the two phases to describe the various mechanisms of mass transfer, the amount of movement and energy. It offers large possibilities for, in particular, to study the effect of interactions between the liquid and solid phases, on the flow and heat transfer into the suspension. The results of recent research work conducted and published by Fagla[9], on suspensions of large spherical hard particles in a solution of Carboxymethylcellulose (C.M.C.) have showed that the heat transfer is better in turbulent than in laminar regime and that this transfer is influenced by the presence of particles.

## 2. MATERIEL and METHODS

### 2.1. Materiel

#### 2.1.1 Loop test

The experimental installation schematized below on face (Cf. Fig. 1) is essentially constituted of a

ISSN 2278-7763

buckle of tests and a vein of experience (5). The installation is composed of a group motor-pump (2), a tubular intersection in graphite (3), an upstream tray, a PVC tube (chloride of polyvinyl) placed after the downstream tray (4), a transparent PMMA tube (poly methacrylate of methyl), a measure vein, a derivation conduct, an electromagnetic flowmeter and a downstream tray (1). The presence of a phase of strong particles sensitive to the mechanical constraints determined the choice of the motor-pump group. The one that we used, is sufficiently powerful to allow the out-flow of very viscous products with debits approaching the 12 $m^3/h$ (speed producing $U_d$ = 4.6 m/s). It is a centrifugal pump with semi-open wheel and with helical rotor in order not to damage the strong phase too quickly. At the pump exit, the mixture inhaled from the downstream tray is pent-up in a graphite tubular intersection, intended to control the temperature of the mixture. The entry temperature of the suspension in the test vein is maintained constant with a precision of 0.2°C. Then, the mixture arrives in an upstream tray intended to absorb throbbings in the out-flow led by the pump to homogenize the strong liquid mixture and the temperature. A chloride polyvinyl tube (P.V.C.) of a length of 34.54 diameters (equivalent to 1.05 m), and another transparent methyl poly methacrylate tube (P.M.M.A.) of a length of 39.87 diameters (equivalent to 1.212 m), disposed successively in series and in the same way diameter (0.0304 m), permit to obtain the dynamic establishment of the out-flow. They are followed by the vein of experience that is also in P.M.M.A. A derivation conduct joins the exit of the upstream tray to the downstream tray; it permits to adapt the flow of the mixture to the conditions of the wanted manipulation. At the exit of the measurement zone, an electromagnetic flowmeter (7), constituted of a cylindrical element made of Teflon and two turntable electrode, measures the flow in real time. A downstream tray, placed at the exit of the vein of experience and of the derivation conduct, aims to calm the out-flow, to assure a minimal load on the pump and to introduce the strong and liquid phases in the conduct. Holds of pressure at the entry and at the exit of the test vein permit the measurement of the pressure drop with the help of a differential pressure sensor (6). The tubes and the veins of experience: To do the measurement of the pressure drop in a conduct, we used a P. M. M. A. tube. Two holds of pressure placed at each extremity of the P. P. M. A. tube permit to do the measurement of pressure drop on a length of 2.225 m. The tubes are adapted to the implementation of various techniques of measurements as the use of the ultrasonic velocimetry with Doppler effect and the laser velocimetry with Doppler effect (LDA). For the tests in an anisotherme situation, one uses a test vein made of copper (total length, 2.16 m) around which a heating thread (Thermocoax) is coiled (5). This vein allows a parietal electrical heating with a density of constant flux (maximal Power is 4126 W); 55 thermocouples inserted in the partition permit to measure the local parietal temperature along the tube made of copper.

### 2. 1.2 Experiment veins with simple and complex geometries

The experiment veins are composed of simple conducts and the vein with complex geometry. They are measuring elements adapted to the measurement technique used.

- **Conduct with simple geometry**

To measure the rheological behavior and the load loss of a mixture in a conduct, it has been placed in the installation a PMMA conduct with an interior diameter of 30 mm in series with the P V C conduct (5) the lengths of which permit the establishment of the regime. Two pressure taps located at each end of the PMMA tube allow the measurement of the pressure drop over a length of 1.90 m (Fig. 1).

- **conduct with complex geometry (as heating measuring section) and tubes**

It is noted that the configuration of this geometry is intended to promote the mixing of mixtures at low Reynolds number and this especially in the recirculation zone which appears and is established downstream of a sudden enlargement. According to some authors, the recirculation zone reaches an average length equal to 10 times the height of the step in a turbulent regime. The recirculation length is reached for a generalized Reynolds number (Reg) which equals 150 in a laminar flow. The length of the chosen mixture being 12 meters, this allows to include an area of maximum heat transfer (Fig. 2). Diameter ratio D1/D2 = 0.5 appeared to be the best compromise

ISSN 2278-7763

between the development of a mixing zone of the suspension and the risk of obstruction related to the presence of hard spheres. The average diameter of the being 4.36 mm, the height of the recirculation zone should provide heating of the spheres. The diameter upstream of the sudden enlargement should neither generate excessive pressure drop, nor encourage the blocking of the pipe with high concentration in solids. The 30 mm diameter conduct is followed by a first sudden enlargement of with a 40 mm diameter. The complex geometry itself is located downstream of this first enlargement. A convergent contracting the passage the diameter to 20 mm precedes a second sudden enlargement with 40 mm diameter (D1/D2 = 0.5). Then the fluid flows through the mixing length of 120 mm (L = 6 D1) before the second convergent which is the entry of the second module. This second module, identical to the first, ends in a convergent followed by a third sudden enlargement with 40 mm diameter (Cf. Fig. 2).

Figures 3a and 3b show the assembly copper for the thermal measurements. S the first copper element . A coil pitch constant throughout the element (3 mm) was used to impose a contant density of heat flux . The heated portions are: the first mixing zone from the sudden enlargement (first module), the convergent-widening (second module) and the second mixing zone to excluded convergent (third section). The two heating elements connected in series are powered by a variable autotransformer delivering a voltage between 0 and 240 volts. Electrical power is measured by a voltmeter and an ampermeter. The second graph shows the location of the thermocouples in the element, indicated by the position given in millimeters relative to the first enlargement.

Schemas Fig. 3a and 3b show the coil of an electrical heating element with a diameter of 1 mm on the copper element. A constant winding pitch on any the element (3 mm) has permit to impose a density of constant wall heat flux. The heated parts are: the first mixing zone from the sudden enlargement (first module), the convergent-widening (second module) and the second mixing zone until excluded convergent (the third module). The two heating elements connected in series are powered by a variable autotransformer delivering a voltage between 0 and 240 volts. Electrical power is measured by a voltmeter and an ammeter. The second scheme shows the location of the thermocouples in the element, indicated by the position given in millimeters relative to the first enlargement.

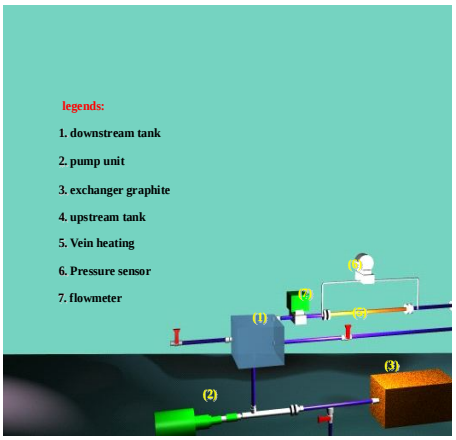


**Fig.1: Schematic of test loop**

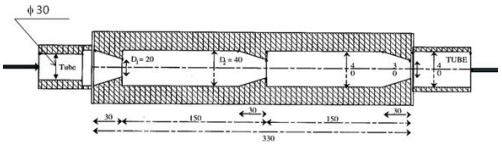


**Fig.2: Complex geometry of the test section.**

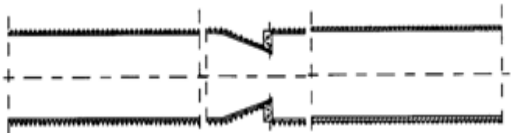

**Fig.3a: Coiling of the heater resistor**

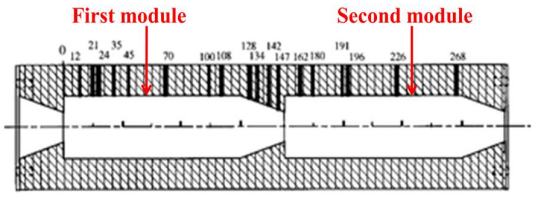


**Fig.3b: Location and grading of thermocouples**

According to Hoareau [5] (see Fig. 4a and 4b), the recirculation zone is being developed in each module for a generalized Reynolds number equal to 100. From Reg = 150, the recirculation zone is fully developed occupying the entire geometry. For Reg ≥ 150, the length of the recirculation zone is constant. Beyond Reg = 550 to Reg = 900, the recirculation zone retracts very rapidly to reach the different lengths in each module: it is the transition from laminar to turbulent flow.

ISSN 2278-7763

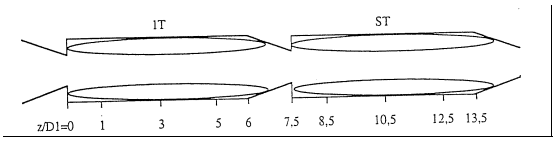


**Fig. 4a: Recirculation zone for Reg ≥ 150 in the complex geometry of the test section**

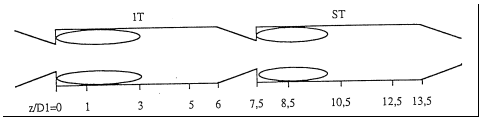


**Fig. 4b: Recirculation zone for Reg 550 ≤ Reg ≤ 900 in the complex geometry of the test section**

### 2.1.3. Fluids and mixtures.

We proceeded to the preparation of solutions at different concentrations Tylose and production of alginate spheres**.**

#### 2.1.3.1. Preparation Tylose at different concentrations.

We prepared a solution of tyloses to 0.4% by mass. To achieve this, we mixed 200 grams of Tylose 50 liters of deionized water. The solution was stirred until homogeneous. To preserve the product we used sodium benzoate. This operation, repeated three times, allowed us to obtain the definitively 150 liters of solution required for installation. To obtain 150 liters of Tylose at 0.75% by mass, it had to realize a mixture with 1125 grams of Tylose.

#### 2.1.3.2. Production of alginate spheres.

The work of **Hoareau** [5] helped us to know the method of manufacture of alginate spheres. A 3% solution of alginate (Protanal LF 10/60 or Protanal SF 120) or 600 grams of Protanal for 20 liters of deionized water. The solution was brewed until complete homogenization. A device allows flowing this solution dropwise into a tank containing a solution of calcium chloride (CaCl2) at a rate of 20 grams per liter. Gout, taking the form of a sphere during free fall, polymerizes on the surface in contact with the saline solution. It takes about 1 hour to ensure a complete polymerization of spheres but their mechanical strength improves as the time spent in the solution is long.

#### 2.1.3.3. Means of measuring

#### 2.1.3.3.1. The flow rate measurement

It is done with an electromagnetic flowmeter which gives a measure based on Faraday's law. A conductive liquid passing through a magnetic field perpendicular induces a voltage on the measuring electrodes. This flowmeter provides an independent measure of the velocity profile, introduces low pressure drop and is not influenced either by the temperature and pressure or by the fluid viscosity. The alginate spheres are conductive the measurement is not affected. The literature cites flow variations over time in solid-liquid flows. Therefore, it is advisable to increase the integration time of the camera to get an average rate stable, after verification of the phenomenon. The interior of the measuring cylinder is coated with Teflon and the electrodes are alloy Hastelloy C.

#### 2.1.3.3.2. Pressure measurement

Pressure measurement is done using the difference of pressure between the catches, situated on both side of the tube PMMA which were obtained using the differential pressure sensors with variable inductance. The sensitive element of the measuring cell consists of a membrane attached to a magnetic core moving through the air gap of two coils. The pressure difference applied on both separating diaphragms is transmitted to the measuring diaphragm by means of a filling liquid. The displacement of the core changes the mutual inductance of the two coils and the potential of the midpoint of these two inductors. This potential change is processed and amplified. A thermal sensor is used to compensate of possible effects due to temperature. The output signal, a 4 to 20 milliampere current is read on a digital display multimeter or converted into 2-10 V signal to be recorded directly to a PC of acquisition. We used a sensor, measuring ranges equal to 500 mbar, can be set to ranges from 1/4 to 1/1 of the maximum pressure difference of with a measurement accuracy of the order of 0.15%. Calibration was performed with columns of water.

### 2.1.2. METHODS

#### 2.1.2.1. Rheological and hydrodynamic studies

Our recent work has shown that the hard spheres have an influence on the longitudinal pressure gradient in laminar regime. Their presence results in an increase of the value of the longitudinal pressure gradient ($\Delta P/L$) and the consistency of the mixtures increases linearly as a function of the volume fraction of hard spheres. According to

ISSN 2278-7763

Hoareau [5] , the figures 2a and 2b show the recirculation zone which is being developed in each module for a generalized Reynolds number of Metzner and Reed with Reg = 100. It is of the form << Eq. (1) >>.

$$\mathrm{Re}' = \rho \overline{U}^{2-n} \frac{D}{K}^{n}$$

(Eq.1)

at Reg = 150, the recirculation zone is fully developed occupying the entire geometry. For Reg = 150, length of the recirculation zone is constant. Beyond Reg = 550 and until Re = 900, the recirculation zone retracts very quickly to reach different lengths in each module. This is the transition from laminar to turbulent. To determine K and n, we used the relationship Rabinowitsch-Mooney applied to the case of a pseudoplastic fluid form << Eq. (2) >> << and Eq. (2 ') >>:

$$\frac{8Q_v}{\pi D^3} = \frac{n}{3n+1}\left(\frac{\tau_p}{K}\right)^{\frac{1}{n}},$$

(ref. Eq.2)

$$\text{with } \tau_p = K\left(\frac{3n+1}{4n}\right)\left(\frac{8\overline{U}}{D}\right)^{n},$$

(ref. Eq.2')

with $Q_v$ : Flow rate and D: the diameter of the measuring section; the parietal constraint is experimentally determined by the relationship << Eq. (3) >>.

$$\tau_p = \frac{\Delta P D_H}{4L},$$

(ref. Eq.3)

with ΔP: pressure drop; $D_H$: hydraulic diameter; L: length of the measuring section

The evolution of the concentration in spheres has no influence on the structure index (n). By against, consistency (K) increases the concentration of in spheres. The influence of the spheres on the longitudinal gradient of pressure results in an increase of the value of ΔP / L in laminar flow and by a transition of dynamic regime earlier and more spread. By against the turbulent regime is independent of the presence of the spheres.

Thus we can affirm that the spheres have an influence on the longitudinal pressure gradient in laminar flow. Their presence results in an increase of the value of the longitudinal pressure gradient (ΔP / L): the consistency of the mixtures increases linearly with the concentration of solid phase. Rheological characteristics values obtained from the controlled stress rheometer are different from those obtained by the measurements of pressure drops. However, a careful examination of rheograms obtained shows that the parameters (n and K) change in the entire range of shear.

### 2.1.2.2. Influence of generalised Reynolds number on the heating

The figure 5 shows the evolution of the average Nusselt number for different values of heat flux. The average Nusselt number changes weakly and linearly for a generalized Reynolds number between 43.8 and 228: It is the laminar flow with a gradual evolution of the Nusselt number. Then we find a sudden change in slope reflects a change in dynamic regime. Here is the case of the transitional regime for Re 'between 590 1028. Between Reg = 1028 and Reg = 1525 we have a new change of slope which reminds us of the early turbulent regime. This is confirmed by the fact that from Reg =900, the recirculation zone retracts, indicating the transition from laminar to turbulent flow.

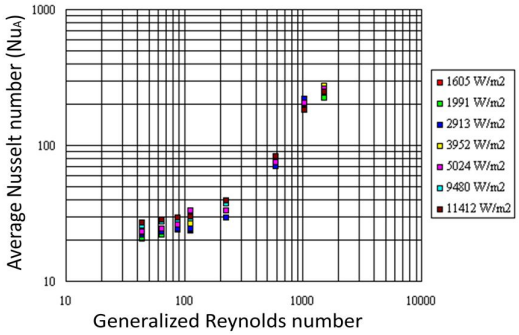


**Fig. 5 : Evolution of the average Nusselt number function of different values of heat flux densities**.

### 2.1.2.2. Thermal Studies - Thermal measurements - Determination of exchange coefficient

Thermal measurements are made by determining the heat transfer coefficient h. The heating power is provided by two heating resistors in series and powered by a single phase variable autotransformer. Iron-Constantan thermocouples of 1 mm diameter are connected to a central thermal measurements whose trademark is Sat AOIP MEASURES 70. The apparatus has 70 input channels and cold junction compensation. We measured the temperature using only 20 channels. This is an apparatus which has analog and digital inputs, relay outputs and analog outputs and a power supply gauge. This allowed us to schedule the start of the scan of the various channels to follow the evolution of the temperature and to determine the thermal equilibrium. The thermocouples installed in wall allow local measurement of convective heat transfer coefficient h(z). The thermocouples installed in the wall allow a local measurement of the convective

ISSN 2278-7763

heat exchange coefficient h (z) and this coefficient is obtained from a thermal balance according to the relation << Eq. (4) >>:

$$h(z) = \frac{\varphi_P}{T_P(z) - T_m(z)}$$

(ref. Eq.4)

The determination of h (z) assumes knowledge of dynamic and thermal fields and resolution of the five equations (one continuity equation, three equations of motion and one for heat equation). Graetz [10] has solved in the Newtonian case neglecting viscous dissipation and radial diffusion in assuming constant parietal temperature $T_p$ or the constant parietal heat flux density $\varphi_p$. The equation is of the form << Eq. (5) >>:

$$\rho C_p u \frac{\partial T}{\partial z} = \frac{\lambda}{r}\frac{\partial}{\partial r}\left(r\frac{\partial T}{\partial r}\right)$$

(ref. Eq.5)

For a Newtonian fluid in laminar flow, the Nusselt number (Nu) which is expressed by << Eq. (6) >>:

$$Nu = \frac{hD}{\lambda}$$

(ref. Eq.6)

It characterizes the amount of heat exchange between wall and the fluid. For a steady state regime, the previous heat equation gives a asymptotic Nusselt number $Nu_\infty$ = 3.66 at Tp equals a constant, and $Nu_\infty$ = 4.36 at $\varphi_p$ = constant. For a Non-Newtonian fluid in established laminar regime, most authors propose a solution Graetz [10] type in which the Non-Newtonian character is reflected in the velocity profile. For a pseudoplastic fluid, Lyche and Bird (1956) propose $Nu_\infty$= 3.949 with n = 1/2 or $Nu_\infty$ =

$$T_m(z) = T_e + (\pi D_2 . \varphi_p / (\dot{M} C_p))z$$

(ref.Eq.10)

The wall temperature Tp (z) is obtained by direct measurement of the different probes.

$T_e$ is the temperature at the inlet of the exchanger,

$$Nu\infty = 8(5n+1)(3n+1)/31n$$

(ref. Eq.11)

Figure 6 shows the evolution of the Nusselt number for a given flux density for different Reynolds number. It shows a significant dependence of the transfer related to the particular dynamics of the flow in this geometry.

### 3. RESULTS AND DISCUSSION

Figure 6 shows the evolution of the Nusselt number for a given flux density at different Reynolds numbers. In this Figure, we see that all the curves dropped to the abscissa z/D = 7.5 at 4.175 with n = 1/3 at Tp = constant and << Eq. (7) >> at $\varphi_p$ = constant :

$$Nu_\infty = \frac{8(5n+1)(3n+1)}{31n}$$

(ref. Eq.7)

Later Bird [11] have proposed << Eq. (8) >> at constant $\varphi_p$ .

$$Nu_\infty = \frac{8(5n+1)(3n+1)}{31n^2+12n+1}$$

(ref. Eq.8)

For our fluid, this value is equal to 5.58 (n = 0.83). We know that the Nusselt number reaches a low point of separation then increases linearly to a maximum at slightly beyond the reattachment zone. This corresponds to the birth of the thermal boundary layer. The heat transfer is maximum and minimum respectively in the immediate vicinity of the points of separation and reattachment.

## 2.1.2.3. Case of single-phase flow.

We worked on a solution of 0.75% Tylose. The heat exchange in a fluid is characterized by the Nusselt number (Nu). The local Nusselt number Nu (z) is given by the following expression << Eq. (9) >>.

$$Nu(z) = \varphi_P D_2 / \left[(T_P(z) - T_m(z))\lambda\right]$$

(ref. Eq.9)

with maximum diameter $D_2$ passing through the geometry downstream of the sudden enlargement ($D_2$ = 0.04 m); Tm (z) is the mixture temperature. It is obtained by expressing the heat balance, neglecting losses outward axial conduction losses in the copper << Eq. (10) >>.

$\dot{M}$ is the mass flow rate, $\varphi_p$ is the density of heat flux. In established thermal regime in the expression of asymptotic Nusselt number is given by << Eq. (11) >>.

the output of the convergent and recovered to the abscissa z/D = 8.5. For a generalized Reynolds number (Reg) between 43.8 and 228, the Nusselt number changes very little. But Reg = 590, the Nusselt number is almost constant until z/D = 1.5 and from z/D = 2, there is an increase that reached a maximum at 5.5 (corresponding to the place entrance of the convergent in the first module: gluing zone that is the seat of best heat exchange, from where the Nusselt number is greater). It falls in the convergent to reach a minimum at the abscissa of the maximum velocity (output convergent). A Reg = 1028, the Nusselt number is much higher. It reaches its

ISSN 2278-7763

maximum and minimum at the same abscissa as the previous curve. A Reg = 1525, the Nusselt number is much higher. We also observe a slight peak at abscissa z / D = 2.45. This slight increase followed by a small fall tells us about reattachment of the first module. A similar situation is observed at the abscissa z / D = 9.8 is the location of reattachment of the second module. The slight peak due to reattachment is also observed on the curve associated with the Reg = 1028.

Moreover, the curves associated respectively with Reg = 43.8; Reg = 65, Reg = 88.3 and Reg = 228 are autosimilar, and suggest us a laminar regime. Curves associated respectively with Reg = 590, Reg = 1028 and Reg = 1525, due to their distance from each other, lead us to conclude that we are in the case of turbulent and transient flows.

For the fluid flowing respectively Reg = 43.8; Reg = Reg = 88.3 and 65 the value of the Nusselt number is low. This is explained by the fact that there is a developped recirculation zone where the heat is minimal in laminar flow. So for Reg = 43.8 the evolution of the Nusselt number has the same shape for different heat flux (see Fig. 7). For heating and suspensions in Figure 7 where Reg = 1028, we find that, from the outset ie z / D = 0, the heat transfer is stronger at 5% than at 10% of solids. This fall of Nusselt at 10% in solid particles was accentuated to z / D1 = 5.5. So at this abscissa all curves have started to fall. They reach their minima in the convergent uniformly and identically. This allows us to say that in the laminar regime, the maximum of Nusselt number is reached at the entrance of the convergent both for the first and for the second modules. We also find that the evolution of the Nusselt number is proportional to the flux density. Nusselt number is a maximum at the entrance of the convergent and fall strongly in the interior of convergent both in the first module in the second.

Figure 8 [for a generalized Reynolds number Reg = 228 (laminar flow)] allows us to appreciate the evolution of of Nusselt number. There was an improvement in the heat transfer. The presence of a quasi developed recirculation zone resulting in a gradual increase in the heat transfer. It reaches its maximum at the abscissa (z / D) between 5 and 6.5 or at the entrance of the first convergent. In the convergent all the curves have fallen identically to a minimum at the abscissa of the maximum velocity. The effects of the temperature dependence are accompanied by a fluidification of the fluid in the region near the wall and an increase in the speed variation. The heat transfer is improved.

In the first module of Figure 9 (with Reg = 1525), the effect of the recirculation zone is reflected in a gradual increase in the of Nusselt number. In the second module, the effect of the recirculation zone is not sensitive: the Nusselt number no longer changes. The entanglement of curves is explained by the turbulent flow. Indeed, from Reg = 900, the recirculation zone is retracted, it is the effects of the turbulent recirculation zone.

By examining precisely the curves of Figure 6 shows that all the curves dropped to the abscissa z / D = 7.5 at the outlet of the convergent and rose again to the abscissa z / D = 8.5.

The small gap that exists between the curve of Reg = 590 and the curves above allows us to affirm that we have a transitional regime. The weak evolution of the Nusselt number for a generalized Reynolds number less than or equal to 113, is reflected by the presence of the recirculation zone not yet fully developed, when the dimensionless number (z / D) is between 0 and 3 (see fig. 6). These results are corroborated by those obtained by Hoareau **[5]**. Thus we can say that the evolution of the Nusselt number is in keeping with the analysis of the flow dynamics.

### 3. 1 Influence of the flux density

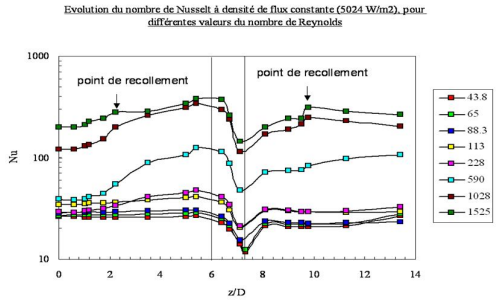


Fig.6 : Evolution of the Nusselt number at constant heat density flux equal 5024 W/m2 for different values of the generalized Reynolds number Reg.

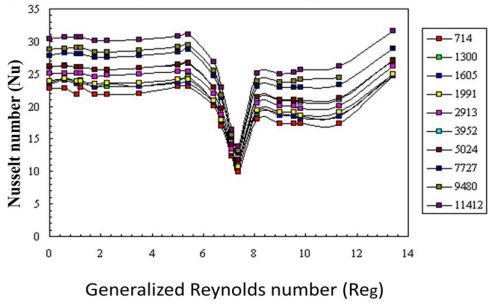


Fig. 7 : Evolution of the Nusselt number as a function of different heat flux for a constant generalized Reynolds number ($Re_g$) equal to 43.8

ISSN 2278-7763

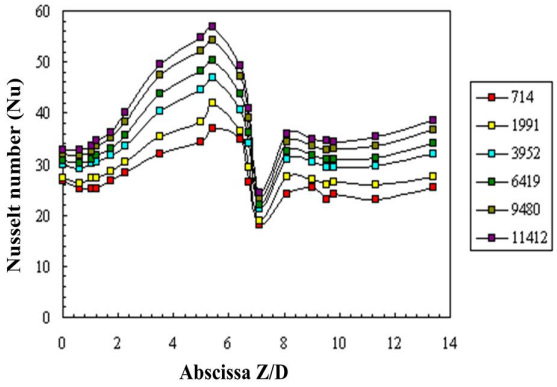


Fig. 8 : Evolution of the Nusselt number as a function different
heat flux for a constant generalized Reynolds number (Reg)
equal to 228.

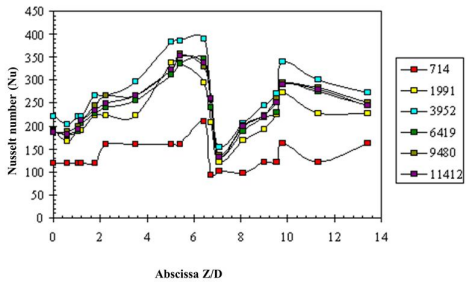


Fig. 9 : Evolution of the Nusselt number as a function different heat flux for a constant generalized Reynolds number (Reg) equal to 1525

### 3.2. Case of two-phase flow

#### 3.2.1. Influence of generalized Reynolds number on the constant heat flux density and constant concentrations spheres

The Figure 10 shows the evolution of the of Nusselt number at constant density and constant mass concentration spheres. In this figure, we see several phenomena:

First, the Nusselt number increases with the constant Reynolds number. Second, the curves whose Reynolds numbers are respectively equal to 590, 1028.4 and 1525.3 dropped to the abscissa z / D = 0.90 before rising. These various falls are explained by a possibly fouling spheres just at backward march. The main vortex becomes the seat of retention spheres that stick together. This creates an increase in the temperature of the wall, due to a fall of of Nusselt number. Third, the abscissa z / D = 1.8, there is the appearance of small elevations for the curves (Reg = 1028.4) and (Reg = 1525.3). They are the impacts which are related to either a breakpoint or shocks of the spheres.

### 3.3. Influence of the concentration of spheres on the heating at constant flux density

The influence of the concentration of the alginate beads on heating between the wall and the mixture in the complex geometry is shown in Figures 11, 12 and 13. At Reg = 590, there is a sharp increase in the Nusselt number in two-phase flow compared to monophasic case. In the downstream of the first sudden enlargement ($0 < z/D < 3$), we note an improvement in the heat transfer which is certainly due to particle-wall interactions. The higher the concentration is , the stronger the transfer is. In the second part of the first module ($3< z/D <6$), we are seeing a tightening phase flow behavior. This last remark is also valid in the second module where, however, for a concentration of spheres $\emptyset = 2.5$, a singular point appears at $z/D = 11$. This is explained by the fact that there are important interactions spheres- wall (see Fig. 11).

At Reg = 1028 (Fig. 12), we find that from the outset $z/D = 0$, the heat transfer is higher at 5% of spheres than 10% beads. This Nusselt number drop at 10% spheres has increased to $z/D = 5.5$ to become lower than the monophasic case. This trend is maintained for the rest of the geometry. The concentration of spheres has less influence on the transfer of heat from a certain threshold. This is undoubtedly due to the too high value of our index structure (close to 0.9).

At Reg = 1525, (Fig. 13) the Nusselt number is very high for concentrations of spheres 2.5% and at 5% and the same way. For against, the Nusselt number at 10% of concentration of alginate beads has continued the trend described above. He became weaker than the monophasic case where $z / D = 7.5$ ie the point of descending march and it makes us think that the saturation increases with increasing generalized Reynolds number.

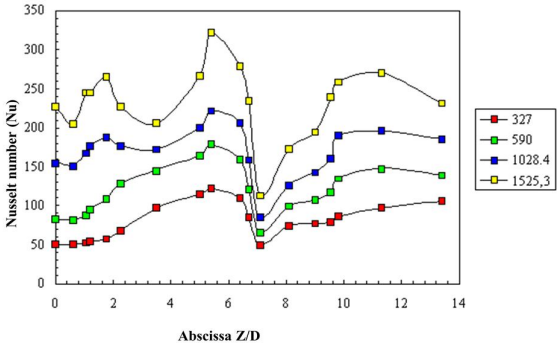


Fig. 10 : Evolution of Nusselt number as a function of constant volume fraction ø= 10% and a constant flux density $\Phi$ = 9480 W/m$^2$.

ISSN 2278-7763

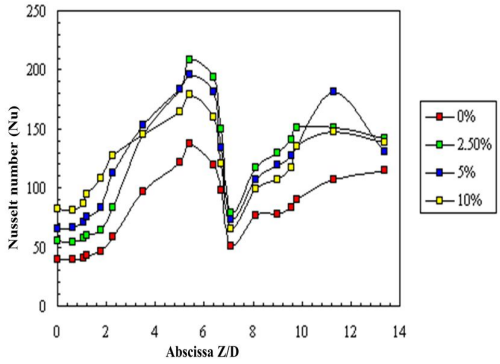


Fig. 11: Evolution of Nusselt number as a function of constant Reynolds number Reg = 590 and a constant flux density $\Phi$ = 9480 W/m$^2$

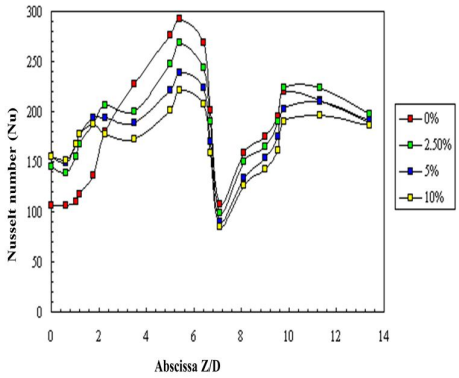


Fig. 12: Evolution of Nusselt number as a function of constant Reynolds number Reg = 1028 and a constant flux density $\Phi$ = 9480 W/m$^2$

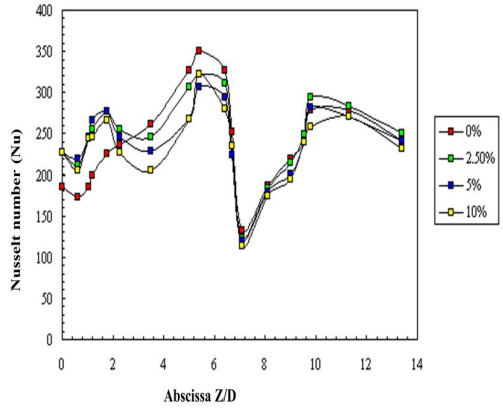


Fig. 13: Evolution of Nusselt number as a function of constant Reynolds number Reg=1525 and a constant flux density $\Phi$ = 9480 W/m$^2$

## 3. Conclusion

As a general remark, in all cases, two-phase flow, there is an improvement in the heat transfer. This is due to particles-wall interactions. The particles are interacting with the wall and they disturb the thermal boundary layer. This is verified experimentally in all cases of figures. We have made the study of heat transfer in the flow of Non-Newtonian fluids and two-phase mixtures in a complex geometry. Experimental means implemented have led us to the results for the flow of solid-liquid suspensions in complex geometries for spherical particles aspect ratio (d / D) greater than 0.13. These means have enabled us to understand the mechanisms of heating the mixture from the wall. We also observed the effect of the concentration of solid spherical particles on the quality of heat transfer with its limitations. We highlighted the improvement of heating by using a complex geometry. It increases the quality of the heat transfer between the mixture and the wall with the birth of a recirculation zone which improves the homogenization of the suspension and shock between the hard spherical themselves. The temperature dependence of the carrier fluid swished from different fluid-particle interactions, particle-wall for the quantification of each phenomenon. In the case where particles are added to the liquid phase is observed in all cases improved heat transfer due to the many interactions "particle-particle", "particle-fluid" and "particle-wall." Understanding of the different interactions are essential.

## REFERENCES

[1] Chhabra, R. P... Motion of spheres in power law (visciinelastic) fluids at intermediate Reynolds numbers: an unified approach, Chem. Eng. Process, Vol.28. pp. 89-94, 1990.

[2] Cheng D.C.-H. A design procedure for pipeline flow of Non-Newtonian dispersed systems. Fluid Mech. Vol.43. pp. 381-384, 1970.

[3] Kemblowski Z, Kolodziejski J. Flow resistance of Non-Newtonian fluids in transitional and turbulent flow Int. Chem. Eng. Vol.13, pp. 265-279, 1973.

[4] Takahashi T. Pressure drop of suspensions in heterogeneous flow, Hydrotransport V, 8-11 May, paper C5. Vol.7 pp. 35-48, 1978.

[5] Hoareau F. Etude dynamique et thermique de suspensions solides-liquides non-newtoniennes en conduite, Université de Nancy I France; 1996. (Thèse)

[6] Fagla FZB. Etude thermique de suspensions solides-liquides non newtoniennes en conduite complexe horizontale, DEA en Mécanique Energétique I.N.P.L. Vandœuvre-lès-Nancy France; 1998.

[7] Fagla F.Z.B., Gradeck M., Baravian C., Lebouché M. ''Etude expérimentale de l'hydrodynamique des suspensions Non-Newtoniennes de «grosses » particules dans une conduite horizontale'', Vol.15, N°1, (Annales des Sciences Agronomiques, pp. 139-157, 2011.

[8] Rhafiki T. El; Schall E. Mimet.; Y. Zeraouli, ''Modélisation et étude numérique d'un écoulement phasique solide-liquide subissant un changement de phase dans un échangeur de chaleur''. Thèse de doctorat, Université de Pau et des Pays de l'Adour et Université Abdel Malek Essaidi,Tetouan, Maroc, vol.1 p.188. 2009.

[9] Fagla B. F. Z., Gradeck M., Baravian C., Lebouché M.. ''Thermal study of the Non Newtonian << solid – liquid >> suspensions based on carboxymethylcellulose in the flow of a horizontal duct'' IJSER, Vol. 4, N° 2, pp. 1-11, 2013.

[10] Graetz L. Uber die Warmeleitungsfahigkeit von Flussigkeiten, Annalen der Physik und Chemie, part 1,: Vol.18. pp. 79-94, 1883.

[11] Lyche BC, Bird RB. The Graetz Nusselt problem for a power law Non-Newtonian fluid, Chem. Eng. Sci., , Vol. 6. pp. 35-39, 1956.